

DEVELOPING AN ASYMPTOTIC THEORY FOR DISTRIBUTED ROUGHNESS

An Undergraduate Research Scholars Thesis

by

MADELINE MCMILLAN

Submitted to the Undergraduate Research Scholars program at
Texas A&M University
in partial fulfillment of the requirements for the designation as an

UNDERGRADUATE RESEARCH SCHOLAR

Approved by Research Advisor:

Dr. Edward White

May 2018

Major: Aerospace Engineering

TABLE OF CONTENTS

	Page
ABSTRACT	1
DEDICATION	2
ACKNOWLEDGMENTS	3
1. INTRODUCTION AND LITERATURE REVIEW	4
1.1 Distributed Roughness - Experimental Background	4
2. INTRODUCTION TO CLASSICAL TRIPLE DECK THEORY	8
2.1 Scaling	9
2.2 Asymptotic Analysis	9
2.3 Information Flow	9
3. TRIPLE DECK SCALING DERIVATION	11
3.1 Blasius Flow	11
3.2 Upper Deck Derivation	14
3.3 Middle Deck Derivation	17
3.4 Lower Deck Derivation	19
4. SUMMARY AND CONCLUSIONS	23
REFERENCES	24

ABSTRACT

Developing an Asymptotic Theory for Distributed Roughness

Madeline McMillan
Department of Aerospace Engineering
Texas A&M University

Research Advisor: Dr. Edward White
Department of Aerospace Engineering
Texas A&M University

Recent experiments have shown how distributed roughness fields have the potential to delay transition caused by large discrete roughness elements. This ‘shielding effect’ seems to indicate a shifting of the boundary layer over the roughness field, allowing protruding roughness elements to extend further into the freestream without causing transition. Currently, no theoretical model exists to correctly describe the flow physics over a distributed roughness field. A model would allow efficient computational study of such fields, as well as enhance understanding of distributed roughness transition mechanisms. Asymptotic analysis, similar to the analysis used to create triple-deck theory, is examined herein for its ability to provide potential scaling solutions to characterize many different types of roughness fields. It is shown herein that previous experiments on distributed roughness fit within the scaling bounds used to characterize triple deck theory, and can therefore be modified and extended to distributed roughness.

DEDICATION

To my parents.

ACKNOWLEDGMENTS

This work is funded by the Air Force Office of Scientific Research through Grant FA9550-15-1-0345.

1. INTRODUCTION AND LITERATURE REVIEW

Transition from laminar to turbulent flow induced by surface roughness has been a subject of study for several decades. The ability to delay this transition has significant implications for skin friction drag on aerodynamic surfaces, i.e. aircraft, wind turbines, etc. Even small surface defects such as insect roughness or surface erosion from weathering can cause premature transition of the boundary layer. Understanding the effects various types of surface roughness have on transition is vital to enhancing our understanding of boundary layer flow physics.

Much of transition research has centered around the problem of 2-D and 3-D discrete roughness elements. The path to transition due to these discrete elements can be adequately understood through the lens of receptivity theory [1] [2]. Equations also exist to accurately predict the disturbances created by a discrete roughness element [3]. However these equations do not extend to the problem of a distributed roughness field. The distributed roughness problem is complicated by the fact that an accepted standard for distributed roughness does not yet exist. Recently, experiments have been performed that show the potential distributed roughness has for delaying roughness induced transition. In order to continue to enhance our understanding of flow physics over roughness, theoretical models for flow over distributed roughness fields must be developed.

1.1 Distributed Roughness - Experimental Background

Early work on the distributed roughness problem began with an experiment conducted by Reshotko and Leventhal [4]. They placed sandpaper roughness on a flat plate, expecting to see a destabilization of Tollmien-Schlichting (TS) waves (a transition mechanism). However, only an outward shift of Blasius flow was observed. Later studies sought to apply ideas from transient growth theory to distributed roughness. The hope was that discrete

roughness theory, appropriately modified, could explain distributed roughness transition. Downs and White [5] placed small amplitude distributed roughness on a flat plate and measured the resulting transient growth in the 2-D boundary layer that. Drews et al. [6] conducted a companion direct numerical simulation (DNS) study. They found that removing some of the smaller height roughnesses caused disturbance amplitudes to increase. The idea that the presence of smaller amplitude roughness around large amplitude roughness could delay transition is known as ‘roughness shielding.’ This finding was confirmed by Kuester and White [7], and again using much larger amplitude roughness by McMillan et al. [8].

The larger amplitude roughness used by McMillan et al., along with the adjustable height discrete roughness elements, illustrated conclusively that current expressions about discrete roughness elements and their impact on flow performance do not hold in a field of distributed roughness. Furthermore, they cannot be used to analyze a field of distributed roughness as though it was broken up into many discrete roughness elements. Figure 1.1 shows the geometry of the roughness (both distributed and discrete) used by McMillan et al. [8]

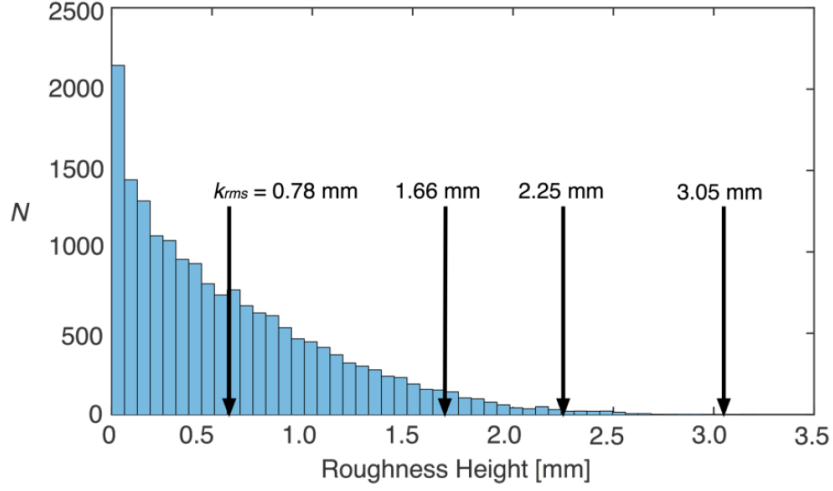


Figure 1.1: Distributed and Discrete Roughness Geometry

We can use a non-dimensional number, Re_{kk} , to describe the height of the roughness element. This number is a good indicator of the effect a discrete roughness element will have on flow transition. The highest point in the distributed roughness field was 3.19 mm, which corresponds to $Re_{kk} \approx 464$, a definite indication of transition for any solitary discrete roughness elements [8]. However, the field merely caused an increase in the velocity fluctuations [8]. A new model must be developed for distributed roughness to help properly predict the effects it has on fluid flow. However, this presents some challenges.

Computational studies of distributed roughness are complex and expensive. To study the roughness used by McMillan et al. would require painstaking effort to properly map the roughness field and then model its effect on the flow. The scale of a boundary layer presents additional problems. Boundary layers over an aircraft wing, which can be tens of meters long, are only centimeters high. Without a good approximation of the flow physics in the boundary layer, high numbers of cells and computational time must be dedicated

to accurately capture the velocity gradients in the boundary layer. It's crucial to get these gradients correct, because drag is directly proportional to the velocity gradient.

Additionally, we cannot know what shape real world distributed roughness will take. It could be insect roughness, ice accumulation, or paint wrinkles. The techniques used in triple deck theory, a mathematical approximation to model disturbances in a flow, offer a way to describe an entire class of flow physics in a relatively simple model. In order to examine the feasibility of a more general model, classic triple deck theory is derived and examined herein.

2. INTRODUCTION TO CLASSICAL TRIPLE DECK THEORY

When solving the Navier-Stokes equations to describe the shape of a boundary layer, only a few exact solutions are possible; These solutions describe very precise scenarios, such as flow in a channel or pipe. One of the precise solutions to the Navier-Stokes equations describes fully developed flow over a semi-infinite flat plate. This flow is described by Blasius flow, and is only valid in a idealized scenario with no disturbances. Once disturbances, such as small bumps or steps, are introduced into the flow, the boundary layer is perturbed and takes on a slightly different shape. Describing the shape of this boundary layer analytically becomes more complicated. Different techniques are needed to approximate the fluid movement.

Triple Deck Theory is a mathematical model that utilizes asymptotic analysis to describe the way disturbances to a flow perturb a Blasius boundary layer. The classic triple deck problem deals with a bump that is specifically sized to just barely cause separated flow in the wake of the bump [9]. This problem cannot be described by classical boundary layer theory because a singularity appears in the equations due to the separated flow (called a Goldstein singularity) [10]. To circumvent this problem, triple deck theory breaks the boundary layer up into three portions, or 'decks'. Each of these decks are analyzed under different scaling conditions. These scaling conditions use the Blasius solution as a basic solution, and allow disturbances caused by the bump to be added in as a perturbations[10]. After solving the different decks, the size of the decks and the shape of the bump can be described relative to the Reynolds number of the flow. This allows a whole class of fluid flow to be analytically described.

2.1 Scaling

Ideally we'd like to identify which terms in a complex equation hold the most influence in a problem, so we can simplify the problem by dropping some terms. We therefore choose scaling terms to use while non-dimensionalizing Navier-Stokes. This same technique is used while deriving the Blasius solution to Navier-Stokes. If the scaling terms are selected carefully, the nondimensional terms will be order one ($\mathcal{O}(1)$), with constant coefficients of varying orders. If coefficients reveal a term to be significantly larger than other terms, the other terms may be dropped away, leaving a simplified expression. In the triple deck problem, scaling is introduced to simplify the problem, as well as reveal on what scales the bump perturbation affects the flow. The issue then arises that all boundary conditions cannot be met by the same scaling. For this reason, multiple decks are introduced, and asymptotic analysis is used.

2.2 Asymptotic Analysis

Asymptotic Analysis is a method that breaks up a problem into parts (i.e. an inner solution and an outer solution), and ensures the original problem and original boundary conditions are satisfied. The solutions can then be superposed to fully describe an approximate solution. This analysis can be done to any degree of accuracy. As more terms are added to the equations, the solution becomes more precise. In triple deck, this allows the different scaling regions to coexist and still form a continuous solution that satisfies all boundary conditions.

2.3 Information Flow

The importance of triple deck is highlighted when examining the way that information moves according to the equations that govern the flow. The full Navier-Stokes equations are elliptic in nature. This means that information introduced in any point in the flow

affects all of the flow, both upstream and downstream of the disturbance. When manipulating the equations to yield the Blasius solution, certain terms are eliminated that enable upstream propagation of disturbance information. Instead of elliptic, the Blasius equation is parabolic so information is only mathematically allowed to move downstream. However, we know intuitively that the flow reacts to a disturbance before reaching it. The triple deck solution allows information about disturbances to move upstream of the disturbance by way of pressure; Information can start off in the lower deck, move upwards through the middle deck, then once in the inviscid outer deck, propagate upstream to inform the incoming flow of the presence of a disturbance [11].

The top deck focuses on flow that is far enough outside the boundary layer to be considered freestream flow. At this height in the fluid, moving away from the wall further will result in no more changes to the flow. This region of the fluid can be considered to be outside the viscous effects caused by the wall, and therefore governed by inviscid flow equations. The lower deck deals with the changes to the velocity profile due to the disturbance. This region is low enough to the wall that the velocity profile in this region can be considered linear. Above this region, in the middle deck, the only change in velocity is the displacement effects causing the velocity profile to shift upwards [10].

3. TRIPLE DECK SCALING DERIVATION

In this chapter the derivation for some important triple deck results will be shown. In each of the decks a different scaling factor will be used.

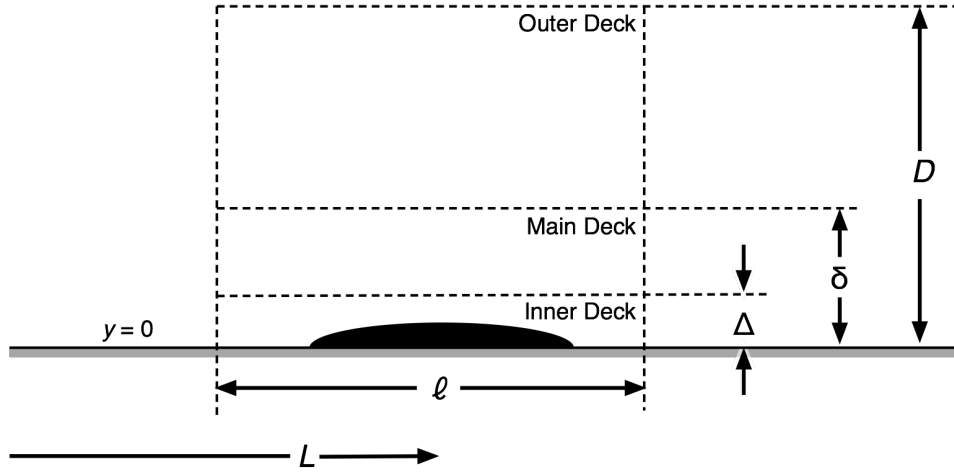


Figure 3.1: Defining Triple Deck Problem Variables

Figure 3.1 shows the geometry of the triple deck problem, along with the variables that will be used in the following derivation. D , δ and Δ are all measured from the ground up to their respective lines. L is measured as distance from the leading edge. l is the distance where the boundary layer is reacting to the presence of the bump.

3.1 Blasius Flow

Because Triple Deck results draw from the Blasius solution as a basic state, it is important to show the results from analyzing the two-dimensional, steady, incompressible Navier-Stokes equations from which Blasius is drawn. Before beginning to non-

dimensionalize the NS equations, scaling must be decided on. The * superscript indicates a dimensional quantity.

$$u = \frac{u^*}{U_\infty} \quad (3.1)$$

$$v = \frac{v^*}{V_{ref}} \quad (3.2)$$

$$x = \frac{x^*}{L} \quad (3.3)$$

$$\eta = \frac{y^*}{\delta} \quad (3.4)$$

$$p = \frac{p^*}{\rho U_\infty} \quad (3.5)$$

L refers to the distance from the leading edge of the flat plate to the point in question, δ refers to the height of the boundary layer, and η is a non-dimensionalized quantity that moves to infinity as the freestream is approached moving away from the plate.

We begin with the continuity equation:

$$\frac{\partial u^*}{\partial x^*} + \frac{\partial v^*}{\partial y^*} = 0 \quad (3.6)$$

By substituting in the scaling in , the following result is obtained:

$$\frac{U_\infty}{L} \frac{\partial u}{\partial x} + \frac{V_{ref}}{\delta} \frac{\partial v}{\partial \eta} = 0 \quad (3.7)$$

By examining the order of magnitude of each of the terms, V_{ref} can be found. The scaling used in this problem was selected such that $\frac{\partial u}{\partial x}$ and $\frac{\partial v}{\partial \eta}$ are $\mathcal{O}(1)$. To match the order of the leading coefficients, V_{ref} is selected to be $\frac{U_\infty \delta}{L}$.

Continuing with the x-momentum equation:

$$u^* \frac{\partial u^*}{\partial x^*} + v^* \frac{\partial u^*}{\partial y^*} = \frac{-1}{\rho} \frac{\partial p^*}{\partial x^*} + \nu \left(\frac{\partial^2 u^*}{\partial x^{*2}} + \frac{\partial^2 u^*}{\partial y^{*2}} \right) \quad (3.8)$$

After substituting the scaling terms and simplifying the equation, the following is found:

$$u \frac{\partial u}{\partial x} + v \frac{\partial u}{\partial \eta} = -\frac{\partial p}{\partial x} + \frac{\nu}{LU_\infty} \frac{L^2}{\delta^2} \left(\frac{\delta^2}{L^2} \frac{\partial^2 u}{\partial x^2} + \frac{\partial^2 u}{\partial y^2} \right) \quad (3.9)$$

By examining the final two terms (the viscous terms) and considering the magnitude of their leading terms, we can drop $\frac{\partial^2 u}{\partial x^2}$. This is because δ , compared to L , is a very small term. When squaring these terms, that difference is exacerbated, and the coefficient becomes much less than 1. By grouping $\frac{LU_\infty}{\nu}$ as a Reynold's number based on L (Re_L), the last term is simplified into the following form:

$$\frac{1}{Re_L} \frac{L^2}{\delta^2} \frac{\partial^2 u}{\partial y^2} \quad (3.10)$$

3.10 shows that $Re_L^{-\frac{1}{2}}$ is scaled with $\frac{\delta}{L}$.

Finally, the y-momentum equation can be examined.

$$u^* \frac{\partial v^*}{\partial x^*} + v^* \frac{\partial v^*}{\partial y^*} = \frac{-1}{\rho} \frac{\partial p^*}{\partial y^*} + \nu \left(\frac{\partial^2 v^*}{\partial x^{*2}} + \frac{\partial^2 v^*}{\partial y^{*2}} \right) \quad (3.11)$$

After substituting in the scaling terms for the Blasius solution, 3.11 becomes

$$u \frac{\partial v}{\partial x} + v \frac{\partial v}{\partial y} = \frac{-L^2}{\delta^2} \frac{\partial p}{\partial y} + \frac{\nu}{U_\infty L} \left(\frac{\partial^2 v}{\partial x^2} + \frac{L^2}{\delta^2} \frac{\partial^2 v}{\partial y^2} \right) \quad (3.12)$$

The same process used for the x-momentum equation can be utilized in the last set of terms for the y-momentum equation. $\frac{L^2}{\delta^2}$ is a large number compared to one, therefore the first viscous term $\frac{\partial^2 v}{\partial x^2}$ is dropped. The resulting simplified expression is as follows:

$$u \frac{\partial v}{\partial x} + v \frac{\partial v}{\partial y} = \frac{-L^2}{\delta^2} \frac{\partial p}{\partial y} + \frac{1}{Re_L} \frac{L^2}{\delta^2} \frac{\partial^2 v}{\partial y^2} \quad (3.13)$$

We know from the x-momentum equation that $\frac{1}{Re_L} * \frac{L^2}{\delta^2}$ is $\mathcal{O}(1)$. Additionally, the two groupings of terms on the left hand side, as well as the remaining viscous term, are $\mathcal{O}(1)$ by design. The only term left for inspection is the pressure term. $\frac{L^2}{\delta^2}$ is very large compared to one. In order to keep the pressure term $\mathcal{O}(1)$, $\frac{\partial p}{\partial y}$ must be very small. This is in good agreement with experiments on Blasius flow; pressure changes in the boundary layer are negligible.

3.2 Upper Deck Derivation

The difference between the triple deck scaling and Blasius scaling comes with regards to the perturbation terms added in the scaling equations. The upper deck will be scaled using the freestream x velocity (U_∞), and consider Blasius flow (denoted by a subscript B) along with perturbations to the flow (denoted by $\hat{\alpha}\hat{\alpha}\hat{\alpha}$).

$$u = \frac{u^*}{U_\infty} = u_B + \epsilon_u u' \quad (3.14)$$

$$v = \frac{v^*}{U_\infty} = \epsilon_v v_B + \epsilon_v v' \quad (3.15)$$

$$x = \frac{x^*}{L} \quad (3.16)$$

$$\xi = \frac{x^*}{l} \quad (3.17)$$

$$Y = \frac{y^*}{D} \quad (3.18)$$

$$p = \frac{p^*}{\rho U_\infty^2} = p_B + \epsilon_p p' \quad (3.19)$$

L is the length from the leading edge of the flat plate to the middle of the bump being analyzed. ξ refers to the length in the x-direction in the immediate vicinity of the bump.

Y is a non-dimensionalized quantity in the y -direction (moving up away from the plate).

First, the continuity equations are analyzed. After substituting in the scaling in 3.14 (scaling factors are carefully selected when splitting derivatives such that the derivative terms remain $\mathcal{O}(1)$) into the continuity equation, 3.6, the following result is obtained:

$$\frac{U_\infty}{L} \frac{\partial u_B}{\partial x} + \frac{U_\infty \epsilon_u}{l} \frac{\partial u'}{\partial \xi} + \frac{U_\infty \epsilon_{vB}}{D} \frac{\partial v_B}{\partial Y} + \frac{U_\infty \epsilon_v}{D} \frac{\partial v'}{\partial Y} = 0 \quad (3.20)$$

Because the solutions to this equation are linear, the terms that appear in the Blasius solution should be dropped out of 3.20; these terms must independently satisfy the equations, which is shown in 3.7. Before they can be dropped, ϵ_{vB} must be selected such that the new coefficients match the Blasius coefficients. ϵ_{vB} is therefore selected to be $\frac{D}{L}$.

In the same way the Blasius leading coefficients were scaled to become $\mathcal{O}(1)$, the upper deck coefficients are also scaled. This yields the result $\frac{\epsilon_u}{\epsilon_v} = \frac{l}{D}$.

Continuing with the x -momentum equation:

$$\begin{aligned} & u_B \frac{\partial u_B}{\partial x} + \frac{u_B \epsilon_u L}{l} \frac{\partial u'}{\partial \xi} + u' \epsilon_u \frac{\partial u_B}{\partial x} + \frac{u' \epsilon_u^2 L}{l} \frac{\partial u'}{\partial \xi} + v_B \frac{\partial u_B}{\partial Y} \\ & + v_B \epsilon_u \frac{\partial u'}{\partial Y} + \frac{v' \epsilon_v L}{D} \frac{\partial u_B}{\partial Y} + \frac{v' \epsilon_v \epsilon_u L}{D} \frac{\partial u'}{\partial Y} = -\frac{\partial p_B}{\partial x} - \frac{\epsilon_p L}{l} \frac{\partial p'}{\partial \xi} \\ & + \frac{1}{Re_L} \left(\frac{\partial^2 u_B}{\partial x^2} + \frac{L^2}{D^2} \frac{\partial^2 u_B}{\partial Y^2} \right) + \frac{\nu L}{U_\infty} \left(\frac{\epsilon_u}{l^2} \frac{\partial^2 u'}{\partial \xi^2} + \frac{\epsilon_u}{D^2} \frac{\partial^2 u'}{\partial Y^2} \right) \end{aligned} \quad (3.21)$$

After dropping the Blasius terms, and rearranging the equation by utilizing the $\frac{\epsilon_u}{\epsilon_v}$ relation found in the continuity equation, the equation simplifies to:

$$\begin{aligned} & u_B \frac{\partial u'}{\partial \xi} + u' \frac{l}{L} \frac{\partial u_B}{\partial x} + u' \epsilon_u \frac{\partial u'}{\partial \xi} + v_B \frac{l}{L} \frac{\partial u'}{\partial Y} + v' \frac{\partial u_B}{\partial Y} + \frac{v' \epsilon_v l}{D} \frac{\partial u'}{\partial Y} \\ & = -\frac{\epsilon_p}{\epsilon_u} \frac{\partial p'}{\partial \xi} + \frac{1}{Re_l} \left(\frac{\partial^2 u'}{\partial \xi^2} + \frac{l^2}{D^2} \frac{\partial^2 u'}{\partial Y^2} \right) \end{aligned} \quad (3.22)$$

At this point, it is important to recall the characteristics of the outer deck. At this height in the boundary layer, u_B is by definition one. Therefore, any derivative terms of u_B are

zero. When we examine the viscous terms, we can see that the coefficient of the $\frac{\partial^2 u'}{\partial Y^2}$ is $\frac{l^2}{D^2}$, which is $\mathcal{O}(1)$. The viscous terms therefore have only $\frac{1}{Re_l}$ as a coefficient, where Re_l is the Reynold's number based on the length scale l . This coefficient is incredibly small, which causes both the viscous terms to drop away. All the ϵ terms are small compared to the flow variables, and at a similar scale to each other, which causes the 3rd and 6th terms in equation 3.22 to drop away. Finally, after noting that $\frac{l}{L}$ is small and drops away, we are left with:

$$\frac{\partial u'}{\partial \xi} = -\frac{\partial p'}{\partial \xi} \quad (3.23)$$

Finally, we look at the y-momentum equation, 3.11. After substituting in the scaling terms, we have:

$$\begin{aligned} & u_B \frac{\partial v_B}{\partial x} + u' \epsilon_u \frac{\partial v_B}{\partial x} + \frac{u_B \epsilon_v L^2}{lD} \frac{\partial v'}{\partial \xi} + \frac{u' L^2 \epsilon_v \epsilon_u}{lD} \frac{\partial v'}{\partial \xi} + v_B \frac{\partial v_B}{\partial Y} \\ & + \frac{v' \epsilon_v L}{D} \frac{\partial v_B}{\partial Y} + \frac{v_B \epsilon_v L}{D} \frac{\partial v'}{\partial Y} + \frac{v' L^2 \epsilon_v^2}{D^2} \frac{\partial v'}{\partial Y} = -\frac{L^2}{D^2} \frac{\partial p_B}{\partial Y} - \frac{\epsilon_p L^2}{D^2} \frac{\partial p'}{\partial Y} \\ & + \frac{1}{Re_L} \left(\frac{\partial^2 v_B}{\partial x^2} + \frac{L^2}{D^2} \frac{\partial^2 v_B}{\partial Y^2} \right) + \frac{\nu L^2}{DU_\infty} \left(\frac{\epsilon_v}{l^2} \frac{\partial^2 v'}{\partial \xi^2} + \frac{\epsilon_v}{D^2} \frac{\partial^2 v'}{\partial Y^2} \right) \end{aligned} \quad (3.24)$$

We can again drop the Blasius terms, and substitute the $\frac{\epsilon_u}{\epsilon_v}$ relation. This yields:

$$\begin{aligned} & u_B \frac{\partial v'}{\partial \xi} + \frac{u' l^2}{L^2} \frac{\partial v_B}{\partial x} + u' \epsilon_u \frac{\partial v'}{\partial \xi} + \frac{v_B l}{L} \frac{\partial v'}{\partial Y} + \frac{v' l}{L} \frac{\partial v_B}{\partial Y} + \frac{v' \epsilon_v l}{D} \frac{\partial v'}{\partial Y} \\ & = -\frac{\epsilon_p}{\epsilon_v} \frac{l}{D} \frac{\partial p'}{\partial Y} + \frac{1}{Re_l} \left(\frac{\partial^2 v'}{\partial \xi^2} + \frac{l^2}{D^2} \frac{\partial^2 v'}{\partial Y^2} \right) \end{aligned} \quad (3.25)$$

Equation 3.25 can be reduced in the same way that equation 3.22 was reduced. The viscous terms again drop away because $\frac{1}{Re_l}$ is a small number. The 3rd and 6th terms drop away due to the ϵ terms being small compared to other flow variables, but the same order of magnitude when compared to each other. $\frac{l}{L}$ is small, which causes the 2nd, 4th and 5th

terms to drop away. Finally, after substituting 1 for u_B , $\frac{l}{D}$, and $\frac{\epsilon_p}{\epsilon_v}$, those simplifications leave:

$$\frac{\partial v'}{\partial \xi} = -\frac{\partial p'}{\partial Y} \quad (3.26)$$

We can take the derivative of equation 3.23 with respect to Y , and the derivative of equation 3.26 with respect to ξ . This leaves us with the following two equations:

$$\frac{\partial}{\partial \xi} \left(\frac{\partial u'}{\partial \xi} \right) = -\frac{\partial^2 p'}{\partial \xi^2} \quad (3.27)$$

$$\frac{\partial}{\partial Y} \left(\frac{\partial v'}{\partial \xi} \right) = -\frac{\partial^2 p'}{\partial Y^2} \quad (3.28)$$

Adding the two right hand sides of equations 3.27 and 3.28 together results in Laplace's equation. The order of derivatives for equation 3.28 can be reversed, and the left hand sides of equations 3.27 and 3.28 can be added together to produce the following:

$$\frac{\partial}{\partial \xi} \left(\frac{\partial u'}{\partial \xi} + \frac{\partial v'}{\partial Y} \right) = \frac{\partial^2 p'}{\partial \xi^2} + \frac{\partial^2 p'}{\partial Y^2} \quad (3.29)$$

Using continuity, equation 3.29 goes to zero, and we are left with the final result:

$$\nabla^2 p' = 0 \quad (3.30)$$

The above form of Laplace's equation is characteristic of inviscid flow which reassures us that our scaling assumptions made for the outer deck were suitable.

3.3 Middle Deck Derivation

The middle deck will be scaled in the following way:

$$u = \frac{u^*}{U_\infty} = u_B + \epsilon_u u' \quad (3.31)$$

$$v = \frac{v^*}{U_\infty} = \epsilon_{vB} v_B + \epsilon_v v' \quad (3.32)$$

$$x = \frac{x^*}{L} \quad (3.33)$$

$$\xi = \frac{x^*}{l} \quad (3.34)$$

$$\eta = \frac{y^*}{\delta} \quad (3.35)$$

$$p = \frac{p^*}{\rho U_\infty^2} = p_B + \epsilon_p p' \quad (3.36)$$

The derivation for the middle deck is very similar to the derivation for the upper deck. The scaling variables D and Y have replaced by δ and η for the middle deck. The continuity result is as follows:

$$\frac{U_\infty}{L} \frac{\partial u_B}{\partial x} + \frac{U_\infty \epsilon_u}{l} \frac{\partial u'}{\partial \xi} + \frac{U_\infty \epsilon_{vB}}{\delta} \frac{\partial v_B}{\partial \eta} + \frac{U_\infty \epsilon_v}{\delta} \frac{\partial v'}{\partial \eta} = 0 \quad (3.37)$$

The terms that appear in the Blasius solution are dropped out of 3.37 after ϵ_{vB} is selected to be $\frac{\delta}{L}$. Additionally, $\frac{\epsilon_u}{\epsilon_v} = \frac{l}{\delta}$.

The new scaling terms are substituted into the x-momentum equation, and yield the following result after all Blasius terms are dropped and the $\frac{\epsilon_u}{\epsilon_v}$ relationship is introduced:

$$\begin{aligned} & u_B \frac{\partial u'}{\partial \xi} + u' \frac{l}{L} \frac{\partial u_B}{\partial x} + u' \epsilon_u \frac{\partial u'}{\partial \xi} + v_B \frac{l}{L} \frac{\partial u'}{\partial \eta} + v' \frac{\partial u_B}{\partial \eta} + \frac{v' \epsilon_v l}{\delta} \frac{\partial u'}{\partial \eta} \\ &= -\frac{\epsilon_p}{\epsilon_u} \frac{\partial p'}{\partial \xi} + \frac{1}{Re_l} \left(\frac{\partial^2 u'}{\partial \xi^2} + \frac{l^2}{\delta^2} \frac{\partial^2 u'}{\partial \eta^2} \right) \end{aligned} \quad (3.38)$$

The assumptions we make at this point are very similar to the assumptions we made for the upper deck. Geometrically speaking, $\frac{l}{L}$ is small, and $\frac{l}{\delta}$ is $\mathcal{O}(1)$. All ϵ terms are small compared to the flow variables, and the same order of magnitude when compared to each

other. Re_l is a large number, and consequently its inverse is very small. Implementing all of these assumptions yields the following result:

$$u_B \frac{\partial u'}{\partial \xi} + v' \frac{\partial u_B}{\partial \eta} = -\frac{\partial p'}{\partial \xi} \quad (3.39)$$

Moving to the y-momentum equation, dropping Blasius terms and substituting the $\frac{\epsilon_u}{\epsilon_v}$ relationship leaves:

$$\begin{aligned} u_B \frac{\partial v'}{\partial \xi} + \frac{u' l^2}{L^2} \frac{\partial v_B}{\partial x} + u' \epsilon_u \frac{\partial v'}{\partial \xi} + \frac{v_B l}{L} \frac{\partial v'}{\partial \eta} + \frac{v' l}{L} \frac{\partial v_B}{\partial \eta} + \frac{v' \epsilon_v l}{\delta} \frac{\partial v'}{\partial \eta} \\ = -\frac{\epsilon_p}{\epsilon_v} \frac{l}{\delta} \frac{\partial p'}{\partial \eta} + \frac{1}{Re_l} \left(\frac{\partial^2 v'}{\partial \xi^2} + \frac{l^2}{\delta^2} \frac{\partial^2 v'}{\partial \eta^2} \right) \end{aligned} \quad (3.40)$$

We can make the exact same assumptions for the y-momentum equation. We end up with:

$$\frac{\partial v'}{\partial \xi} = \frac{-\partial p'}{\partial \eta} \quad (3.41)$$

The middle deck provides very little new information as to the size of terms. It's main purpose is to facilitate the movement of information up from the viscous lower deck to the inviscid upper deck.

3.4 Lower Deck Derivation

For the lower deck we will take a slightly different approach to selecting our scaling terms. We know that this deck is the linear portion of the boundary layer. The Blasius solution actually has set terms that describe the slope of the boundary layer right against the wall. These terms are scaled with η , the middle deck y scaling term. We can use this to our advantage by initially describing our lower deck as a linear dependence on η , with a perturbation. To adjust this value to the lower deck, we can use the definition of η in equation 3.35, along with our new definition of γ , the lower deck y scaling term:

$$\gamma = \frac{y^*}{\Delta} \quad (3.42)$$

By rearranging equations 3.35 and 3.42, we can make the following substitution:

$$\eta = \frac{\Delta}{\delta} \gamma \quad (3.43)$$

In a similar fasion, we can substitute our scaling terms into the Blasius solution for y velocity. We can drop the linear portion of the pressure scaling terms, however we still must have a pressure disturbance to move information. This leaves us with the following lower deck scaling:

$$u = \frac{u^*}{U_\infty} = \frac{\lambda \Delta \gamma}{\delta} + \epsilon_u u' \quad (3.44)$$

$$v = \frac{v^*}{U_\infty} = \frac{\Delta^2}{4 * L * \delta} \gamma^2 + \epsilon_v v' \quad (3.45)$$

$$x = \frac{x^*}{L} \quad (3.46)$$

$$\xi = \frac{x^*}{l} \quad (3.47)$$

$$\eta = \frac{y^*}{\Delta} \quad (3.48)$$

$$p = \frac{p^*}{\rho U_\infty^2} = \epsilon_p p' \quad (3.49)$$

Proceeding as usual with continuity:

$$\frac{U_\infty \lambda \Delta}{\delta L} \frac{\partial \gamma}{\partial x} + \frac{U_\infty \epsilon_u}{l} \frac{\partial u'}{\partial \xi} + \frac{\Delta^2}{4 L \delta} \frac{\partial \gamma^2}{\partial y^*} + \frac{U_\infty \epsilon_v}{\Delta} \frac{\partial v'}{\partial \gamma} = 0 \quad (3.50)$$

The partial of γ with respect to x we can drop immediately as identically zero. This leaves us with the relationship $\frac{\epsilon_u}{\epsilon_v} = \frac{l}{\Delta}$.

After substitution of the scaling terms in the x-momentum equation, we find:

$$\begin{aligned} \lambda \gamma \frac{\partial u'}{\partial \xi} + \epsilon_u \frac{\delta}{\Delta} u' \frac{\partial u'}{\partial \xi} + \frac{l}{4L} \gamma^2 \frac{\partial u'}{\partial \gamma} + v' \lambda + \frac{\epsilon_v l \delta v'}{\Delta^2} \frac{\partial u'}{\partial \gamma} \\ = -\frac{\delta}{\Delta} \frac{\epsilon_p}{\epsilon_u} \frac{\partial p'}{\partial \xi} + \frac{\nu}{U_\infty} \left(\frac{\epsilon_u}{l^2} \frac{\partial^2 u'}{\partial \xi^2} + \frac{\epsilon_u}{\Delta^2} \frac{\partial^2 u'}{\partial \gamma^2} \right) \end{aligned} \quad (3.51)$$

We can immediately drop the γ^2 term because $\frac{l}{L}$ is very small. Because we wish to keep these equations linear, we drop the $u' \frac{\partial u'}{\partial \xi}$ and $v' \frac{\partial u'}{\partial \gamma}$ by limiting our analysis to disturbances that conform to $\epsilon_u \ll \frac{\Delta}{\delta}$ and $\epsilon_v \ll \frac{\Delta^2}{l\delta}$. We also will drop $\frac{\partial^2 u'}{\partial \xi^2}$, because $\frac{l^2}{\Delta^2}$ is much bigger than 1. We end up with:

$$\lambda \gamma \frac{\partial u'}{\partial \xi} + v' \lambda = -\frac{\delta}{\Delta} \frac{\epsilon_p}{\epsilon_u} \frac{\partial p'}{\partial \xi} + \frac{\delta}{\Delta} \frac{1}{Re_l} \frac{l^2}{\Delta^2} \frac{\partial^2 u'}{\partial \gamma^2} \quad (3.52)$$

The first term in equation 3.52 we will consider to be the leading order term. To match the right hand side terms to $\mathcal{O}(1)$, we will choose the magnitude of ϵ_p to be of the same order as $\epsilon_u \frac{\Delta}{\delta}$. Additionally, we can use the relation $\frac{\delta}{L} \approx Re_L^{-\frac{1}{2}}$ to rearrange the coefficients of the viscosity term to show:

$$\frac{\Delta^3}{L^3} \approx \frac{\frac{l}{L}}{Re_L^{\frac{3}{2}}} \quad (3.53)$$

which describes humps that have a length scale of $\frac{l}{L} \approx \mathcal{O}(Re^{-\frac{3}{8}})$, and a lower deck height of approximately $\frac{\Delta}{L} \approx \mathcal{O}(Re^{-\frac{5}{8}})$. Treating the y-momentum equation in a similar fashion, we show that:

$$\lambda \gamma \frac{\partial v'}{\partial \xi} = -\frac{\epsilon_p}{\epsilon_v} \frac{l \delta}{\Delta^2} \frac{\partial p'}{\partial \gamma} + \frac{1}{Re_l} \frac{\delta}{\Delta} \frac{l^2}{\Delta^2} \frac{\partial^2 v'}{\partial \gamma^2} \quad (3.54)$$

We can use the relations found from continuity and x-momentum to reduce equation 3.54 down further to yield:

$$\lambda\gamma = -\frac{l^2}{\Delta^2} \frac{\partial p'}{\partial \gamma} + \frac{\partial^2 v'}{\partial \gamma^2} \quad (3.55)$$

which, due to the magnitude of $\frac{l^2}{\Delta^2}$, shows that $\frac{\partial p'}{\partial \gamma} \approx 0$.

4. SUMMARY AND CONCLUSIONS

In the previous chapter, the derivation for the triple deck problem was shown. We ended with the following results:

$$\frac{l}{L} = Re_L^{-\frac{3}{8}}, \frac{\delta}{L} = Re_L^{-\frac{1}{2}}, \frac{\Delta}{L} = Re_L^{-\frac{5}{8}} \quad (4.1)$$

$$\epsilon_u \approx \frac{\Delta}{\delta}, \epsilon_v \approx \frac{\Delta^2}{L\delta} \quad (4.2)$$

Returning to the experiment done by McMillan et al., we can check that the distributed roughness fits within the bounds that triple deck describes. McMillan et al. performed their experiment at $Re_L \approx 220,000$ [8]. We can rearrange the equations in equation 4.1 to find the order of magnitude for acceptable disturbances. For triple deck to apply to a problem, a disturbance must be smaller than $Re_L^{-\frac{1}{8}}$. For the McMillan et al. experiment, $Re_L^{-\frac{1}{8}} = .21488$, which yields a lower deck height of roughly 3.22 mm (assuming $\delta_{99} \approx 15$ mm) [8]. In the distributed roughness field used by McMillan et al., the tallest peak in the field of distributed roughness was 3.19 mm [8]. The root mean squared height of the field was 0.78 mm [8]. This geometry fits comfortably within the bounds described by triple deck. This suggests that by choosing different scaling terms a reasonable model for a distributed roughness field may be possible using triple deck theory and techniques.

REFERENCES

- [1] Morkovin, M. V. *On the many faces of transition*. CS Wells, 1969.
- [2] Saric, W. S., Reed, H. L., and Kerschen, E. J. “Boundary-layer receptivity to freestream disturbances.” *Annual review of fluid mechanics*, vol. 1, no. 1, (2002), pp. 291–319.
- [3] Tani, I. “Boundary-layer transition.” *Annual Review of FLuid Mechanics*, vol. 1, no. 1, (1969), pp. 169–196.
- [4] Reshotko, E. and Leventhal, L. “Preliminary experimental study of disturbances in a laminar boundary layer due to distributed surface roughness.” *AIAA Paper 81-1224*.
- [5] Downs, R. S., White, E., and Denissen, N. “Transient growth and transition induced by random distributed.” *AIAA Journal*, vol. 46, no. 2, (2008), pp. 451–462.
- [6] Drews, S., III, R. S. D., Doolittle, C., Goldstein, D., and White, E. “Direct numerical simulations of flow past random distributed roughness.” *AIAA Paper 20110564*.
- [7] Kuester, M. S. and White, E. B. “Roughness receptivity and shielding in a flat plate boundary layer.” *Journal of Fluid Mechanics*, vol. 777, (2015), pp. 430–460.
- [8] McMillan, M. N., Berger, A. R., and White, E. B. “Measurements of distributed roughness receptivity.” *AIAA Paper 2017*.
- [9] F. T. Smith, R. I. S. “A two-dimensional boundary layer encountering a three-dimensional hump.” *Journal of Fluid Mechanics*, vol. 83, (1977), pp. 163–176.
- [10] Schlichting, H. and Gersten, K. *Boundary Layer Theory*. Springer, 8th ed., 2001.

- [11] Smith, F. T. “Laminar flow over a small hump on a flat plate.” *Journal of Fluid Mechanics*, vol. 57, (1973), pp. 803–824.